



<b>Title</b>	<b>A study on metal-insulator-silicon hydrogen sensor with La<sub>2</sub>O<sub>3</sub> as gate insulator</b>
<b>Author(s)</b>	<b>Chen, G; Lai, PT; Yu, J</b>
<b>Citation</b>	<b>The 10th IEEE International Conference on Solid-State and Integrated Circuit Technology (ICSICT 2010), Shanghai, China, 1-4 November 2010. In Conference Proceedings, 2010, p. 1465-1467</b>
<b>Issued Date</b>	<b>2010</b>
<b>URL</b>	<b><a href="http://hdl.handle.net/10722/160263">http://hdl.handle.net/10722/160263</a></b>
<b>Rights</b>	<b>International Conference on Solid-State and Integrated Circuit Technology Proceedings. Copyright © IEEE.</b>

# A Study on Metal-Insulator-Silicon Hydrogen Sensor with $\text{La}_2\text{O}_3$ as Gate Insulator

Gang Chen<sup>1</sup>, P.T. Lai<sup>1\*</sup>, Jerry Yu<sup>2</sup>

<sup>1</sup> Department of Electrical and Electronic Engineering, The University of Hong Kong, Hong Kong

<sup>2</sup> School of Electrical and Computer Engineering, RMIT University, Melbourne, Australia

\*Email: laip@eee.hku.hk

## Abstract

A new MIS Schottky-diode hydrogen sensor with  $\text{La}_2\text{O}_3$  as gate insulator was fabricated. Its hydrogen-sensing properties were studied from room temperature (RT) to 300°C. Results showed that the device had excellent hydrogen-sensing performance below about 250°C.

## 1. Introduction

Hydrogen can be converted to electricity, which can be stored in fuel cells, for a great variety of applications. [1] It is the most attractive future energy source. Recent interest in hydrogen has been largely a result of its use as a clean source of energy. However, manipulation and storage of hydrogen are associated with danger of leakage, which can lead to an explosive atmosphere if the hydrogen volume concentration exceeds 4%. [2]

For this reason, it has become very important to develop highly sensitive hydrogen detectors to prevent accidents due to  $\text{H}_2$  gas leakage, thus saving lives and equipment. Catalytic effects play an important role in the field of gas detection [3]. The most common catalysts used for hydrogen sensors are platinum (Pt) and palladium (Pd) [3, 4].

High-dielectric constant (high-k) materials as alternative gate dielectric have attracted much attention to overcome the large leakage current of conventional ultrathin  $\text{SiO}_2$ . Lanthanum oxide ( $\text{La}_2\text{O}_3$ ) is a strong candidate for next-generation high-k gate insulator because of its large bandgap (5.5 ~ 6.4 eV), lowest lattice energy among rare-earth oxides (12400 ~ 12600 kJ/mol), and relatively high dielectric constant (27 ~ 30) [5, 6].

## 2. Experiment

Hydrogen sensor with the structure shown in Fig. 1 was fabricated. The n-type Si (100) substrate ( $0.5\text{-}0.7 \Omega \cdot \text{cm}$ ) was cleaned in acetone in a pyrex glass beaker for 5 min. This was followed by rinsing in isopropanol for 2 min and DI water. The native oxide layer on the Si substrate was removed by dipping in 5% hydrofluoric acid for 10 sec. Subsequently, the Si substrate was rinsed in DI water and blown dry with nitrogen gas.

A 40-nm Ti layer and a 100-nm Pt layer were then deposited in sequence on the back of the Si substrate by DC sputtering of Ti and Pt, respectively to form an ohmic contact. A second cleaning process followed. Since the deposition caused a growth of a thin native oxide layer on the surface of the Si substrate, the native oxide layer was removed with a dipping in 5% hydrofluoric acid for 10 sec. The Si substrate was then cleaned in DI water and blown dry with nitrogen gas.

The gate insulator, a 4-nm  $\text{La}_2\text{O}_3$  layer, was deposited at room temperature by RF sputtering of  $\text{La}_2\text{O}_3$  in a mixed Ar/ $\text{O}_2$  ambient (Ar to  $\text{O}_2$  ratio = 4:1). The front electrode, a 100-nm Pt layer with a diameter of 0.5 mm, was then deposited on the gate insulator by DC sputtering of Pt through a stainless-steel shadow mask. Finally, the sample underwent an annealing in a furnace at 500°C in nitrogen gas (1000 ml/min) for 30 min.

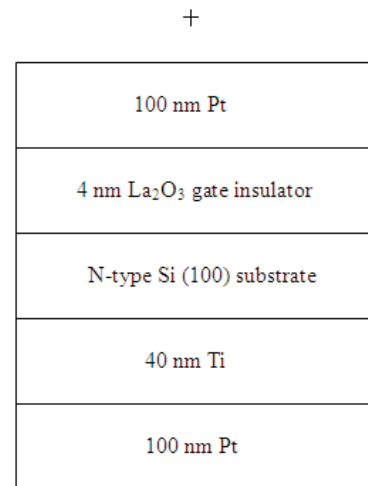


Fig. 1 Structure of the hydrogen sensor

After fabrication of the hydrogen sensor, its hydrogen-sensing properties were studied. Measurements were carried out using a computer-controlled measurement system described in Fig. 2. A thermostat, a semiconductor parameter analyzer (HP4145B) and two digital gas flow controllers (DGFC) were connected to a computer and controlled by software programs. The test sample was placed in a stainless-steel closed chamber inside the thermostat, and gases

were injected into the chamber through the digital gas flow controllers.

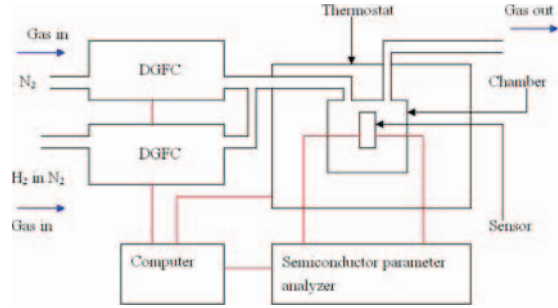


Fig. 2 Computer-controlled measurement system

### 3. Discussion

The sensitivity vs. hydrogen concentration characteristics of the sensor are depicted in Fig. 3, with sensitivity defined as

$$(I_{H_2} - I_{air})/I_{air} \quad (1)$$

where  $I_{H_2}$  and  $I_{air}$  are the currents of the sensor measured in hydrogen and air respectively. As can be seen, the sensitivity increases when the hydrogen concentration increases for each temperature. This is due to an increase of the current in the hydrogen-containing ambient caused by a lowering of the Schottky barrier at the Pt/La<sub>2</sub>O<sub>3</sub> interface. The hydrogen-sensing mechanism is interpreted as follows [7, 8]. First, hydrogen molecules are dissociated to hydrogen atoms by the catalytic metal Pt. Then, hydrogen atoms diffuse toward the Pt/La<sub>2</sub>O<sub>3</sub> interface. The accumulated hydrogen atoms form a dipolar layer to build a local electric field, and thus lower the Schottky barrier height, resulting in a current increase.

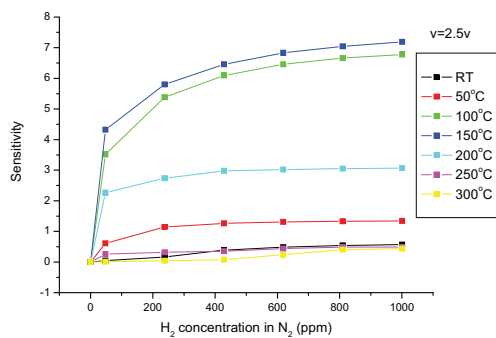


Fig. 3 Sensitivity vs. hydrogen concentration characteristics of the sensor

The hydrogen adsorption activation energy of the sensor can be derived by extracting the slope from the Arrhenius plot of current variation rate ( $\Delta I/\Delta t$ ) versus the inverse of temperature ( $1/T$ ). The activation energy is determined based on the highest current variation rate in first 30 sec upon exposure to 800 ppm H<sub>2</sub>/N<sub>2</sub> for a temperature

range from RT to 200 °C. The resulting Arrhenius plot yields an activation energy of 10.9 kcal/mol for the studied sensor.

Fig. 4 depicts the sensitivity-temperature characteristics of the sensor. The sensitivity initially increases and achieves its maximum at 150°C, but then decreases as the temperature further increases. This phenomenon can be explained as follows [9-11]. When temperature increases (RT ~ 150°C), hydrogen molecules under higher pressure bombard the surface of the electrode more frequently. Hence, more hydrogen molecules can adsorb at the surface of the electrode and also decompose faster into hydrogen atoms, giving higher sensitivity. On the other hand, the oxygen attached to the surface of the electrode (when the sensor is exposed to air) can react with the hydrogen atoms to form hydroxyl ions and water. The formation rates of these products increase rapidly at high temperature, thus decreasing the sensitivity. In addition, further increasing the operating temperature (150°C ~ 200°C) (actually the gas sensor was thermally damaged at about 250°C, and so both 250°C and 300°C were not considered), more electronic defects in the gate insulator are thermally activated and contribute to electrical conduction in the device. As a result,  $I_{air}$  increases more than  $I_{H_2}$  and thus the sensitivity decreases.

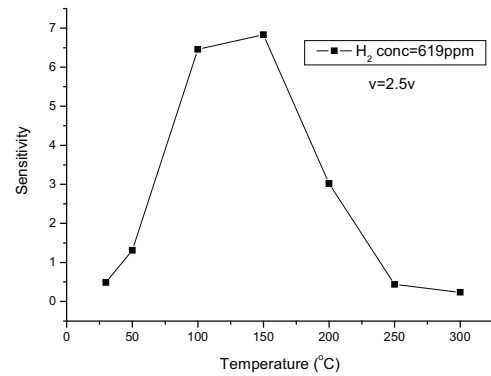


Fig. 4 Sensitivity vs. temperature characteristics of the sensor

The Schottky barrier height ( $\Phi_b$ ) can be calculated as

$$\Phi_b = (K_B T/q) \ln(AA^{**} T^2/I_0) \quad (2)$$

where  $K_B$  is the Boltzmann constant;  $T$  is the absolute temperature;  $A$  is the Schottky contact area;  $A^{**}$  is the effective Richardson constant; and  $I_0$  is the saturation current. The Schottky barrier height variation ( $\Delta\Phi_b$ ) is defined as

$$\Delta\Phi_b = \Phi_b(\text{air}) - \Phi_b(\text{H}_2) \quad (3)$$

where  $\Phi_b(\text{air})$  is the Schottky barrier height in air, and  $\Phi_b(\text{H}_2)$  is the Schottky barrier height in the hydrogen-containing ambient.  $I_0$  (in air or in H<sub>2</sub>)

can be found from the corresponding y-intercept of the graph of  $\ln(I)$  versus  $V$ , and then  $\Phi_b$  can be calculated using the equation (2). As a result,  $\Delta\Phi_b$  can be found from (3).

The barrier-height variation  $\Delta\Phi_b$  vs. hydrogen concentration characteristics of the sensor are described in Fig. 5. In general,  $\Delta\Phi_b$  has an upward trend from RT to 150 °C. As mentioned earlier, the Schottky barrier height is lowered in the hydrogen-containing ambient. Therefore,  $\Delta\Phi_b$  increases as  $H_2$  concentration increases. It is known that the operating temperature of the gas sensor using silicon substrate is limited to below about 250°C [12], primarily due to the small bandgap of silicon.[13] We can see from Fig. 5 that at 200°C,  $\Delta\Phi_b$  decreases slightly when  $H_2$  concentration increases, but it is still positive. Moreover,  $\Delta\Phi_b$  becomes negative at 250°C and 300°C. This phenomenon renders the silicon substrate incapable for use in high-temperature environment.

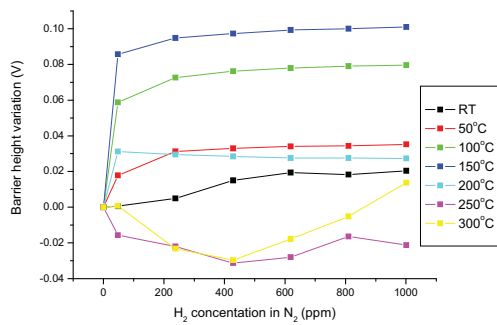


Fig. 5 Barrier-height variation vs. hydrogen concentration characteristics of the sensor

From RT to 200°C, the barrier-height variation vs temperature characteristics (Fig.6) of the sensor are similar to the sensitivity vs. temperature characteristics (Fig.4). They share the same explanations as indicated above.

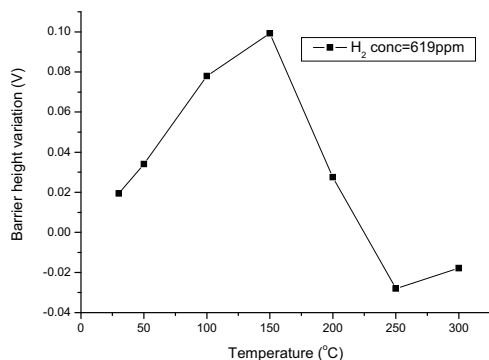


Fig. 6 Barrier-height variation vs. temperature characteristics of the sensor

#### 4. Summary

Metal-insulator-silicon hydrogen sensor with  $La_2O_3$  as gate insulator shows promising hydrogen-sensing properties below about 250°C. A hydrogen adsorption activation energy of 10.9 kcal/mol is obtained for the sensor.

#### Acknowledgements

We would like to acknowledge the University Development Fund (Nanotechnology Research Institute, 00600009) of the University of Hong Kong.

#### References

- [1] J. Villatoro, D. Luna-Moreno and D. Monzon-Hernandez, *Sensors and Actuators B*, 110, p.23 (2005).
- [2] A. Trinchi, W. Wlodarski and Y.X. Li, *Sensors and Actuators B*, 100, p.94 (2004).
- [3] C. Christofides and A. Mandelis, *Journal of Applied Physics*, 68, p.R1 (1990).
- [4] W.C. Hsu, C.C. Chan, C.H. Peng and C.C. Chang, *Thin Solid Film*, 516, p.407 (2007).
- [5] S.-i. Ohmi, C. Kobayashi, K. Aizawa, S. Yamamoto, E. Tokumitsu, H. Ishiwara and H. Iwai, *Proceeding of the 31st European Solid-State Device Research Conference*, p.235 (2001).
- [6] E. Miranda, J. Molina, Y. Kim and H. Iwai, *Microelectronics Reliability*, 45, p.1365 (2005).
- [7] C.W. Hung, H.L. Lin, H.I. Chen, Y.Y. Tsai, P.H. Lai, S.I. Fu and W.C. Liu, *IEEE Electron Device Letters*, 27, p.951 (2006).
- [8] T.H. Chou, Y.K. Fang, Y.T. Chiang, K.C. Lin, C.I. Lin, C.H. Kao and H.Y. Lin, *IEEE Electron Device Letters*, 29, p.1232 (2008).
- [9] W.M. Tang, PhD thesis at The University of Hong Kong (2008).
- [10] C.C. Cheng, Y.Y. Tsai, K.W. Lin, H.I. Chen and W.C. Liu, *Applied Physics Letters*, 86, p.112103 (2005).
- [11] X.F. Chen, W.G. Zhu and O.K. Tan, *Materials Science and Engineering B*, 77, p.177 (2000).
- [12] C.K. Kim, J.H. Lee, Y.H. Lee, N.I. Cho and D.J. Kim, *Sensors and Actuators B*, 66, p.116 (2000).
- [13] A. Trinchi, S.Kandasamy and W.Wlodarski, *Sensors and Actuators B*, 133, p.705 (2008).